ISSN: 0067-2904

Synthesis, Identification and Biological Study of New Pharmaceutical Model Based on Amino Acids with Some of Its Complexes

Simaa Safaa Mahmoud*, Asmaa Mohammed Noori Khaleel
Department of Chemistry, College of Science, University of Baghdad, Baghdad, Iraq

Received: 18/10/2022 Accepted: 16/1/2023 Published: 30/11/2023

Abstract

The synthesis of the MBIB ligand by the reaction of the BIB ligand with methionine in 1:1 ratio, and the metal complexes with Ni(II), Cu(II), and Pt(IV) were described. All synthesized compounds were characterized using spectroscopic methods such as FT-IR, ^{1}H NMR, UV-VIS, thermal analysis (TG and DSC), atomic absorption (AAS), elemental microanalysis (C.H.N.S), melting point (m.p.), magnetic susceptibility, molar conductivity measurements, and chloride content. All the complexes were electrolytes, and the suggested geometric shapes for the complexes were octahedral. The magnetic properties of the platinum complex were diamagnetic, while those of the nickel and copper complexes were paramagnetic. All synthesized compounds have good anti-biofilm properties against bacteria (*Pseudomonas auroginosa*, a gram-negative bacteria), except for C_1(Ni), which is inactive against the same bacteria. In addition, the ligand was evaluated as an anti-cancer agent against human breast cancer (MCF-7), but its effectiveness has been shown to be less effective compared to metronidazole.

Keywords: Metronidazole, Boric acid, Methionine, Antibiofilm.

تحضير، تشخيص و دراسة بايولوجية لموديل دواء جديد يعتمد على الحوامض الامينية مع بعض معقداته

سيماء صفاء محمود*، أسماء محمد نوري خليل
قسم الكيمياء، كلية العلوم، جامعة بغداد، بغداد، العراق

الخلاصة

تم وصف تحضير الليكاند MBIB بتفاعل ليكاند BIB مع الميثيونين بالنسبة المولية (1:1)، أيضا المعقدات الفلزية مع Ni(II)، Cu(II)، Pt(IV) حضرت و شخصت بواسطة الطرق الطيفية: FT-IR، ^{1}H NMR، التحليل الحراري (TG&DSC)، UV-VIS، الامتصاص الذري (AAS) والتحليل الدقيق للعناصر (C.H.N.S)، قياس درجة الانصهار(m.p.)، الحساسية المغناطيسية، التوصيلية المولارية ومحتوى الكلور. كل المعقدات كانت الكتروليتية و الأشكال المقترحة كانت ثمانية السطوح. معقد البلاتين كان دايامغناطيسي بينما معقدات النيكل و النحاس كانت بارامغناطيسية. كل المركبات المحضرة لها فعالية جيدة ضد الغشاء الحيوي لبكتريا((G-) *Pseudomonas auroginosa*) باستثناء C_1(Ni) غير نشط ضد البكتيريا نفسها. أيضا تم تقيم فعالية الليكاند كمضاد لسرطان الثدي ولكن ثبت أن فعاليته أقل مقارنة بالميترونيدازول.

1. Introduction

* Email: saimaa.safaa1205m@sc.uobaghdad.edu.iq

Metronidazole (MTN) is one of several drugs with an imidazole ring [1]. MTN is a preferred drug because it is used in both human and veterinary medicine. It is used to treat diseases caused by anaerobic bacteria and protozoa [2]. Metronidazole has been studied for its antibacterial activity against gram-negative aerobes and some gram-positive bacteria [3]. Boric acid (also called boracic acid or orthoboric acid) is a very weak inorganic acid [4]. Boric acid is extensively utilized in the pharmaceutical and chemical industries; it is widely used as an antiseptic, in eye wash preparation, as an insecticide, and as a buffering agent [5]. Methionine (Met) is one of the nine amino acids that humans essentially must have for healthy growth and tissue repair. Methionine is utilized as a nutritional element in parenteral nutrition, health foods, infant milk preparations, and sports supplements [6]. Methionine is important for the growth of cancer cells and the inhibition of cancer cells. Methionine restriction appears to prevent the growth of cancer cells and may enhance the efficacy of chemotherapeutic medicines, according to a growing body of evidence [7]. In this work, the MBIB ligand will be synthesized by the reaction of a metronidazole derivative with methionine (Figure 1). Following this, metal complexes of MBIB with Ni(II), Cu(II), and Pt(IV) metal ions will be formed (Figure 2). All the prepared compounds will be characterized using physicochemical and spectral analyses. The biological and medicinal activities of the prepared compounds will be evaluated.

2. Experimental part

2.1. Materials

All chemicals were used as supplied (utilizing Hayman, Fieser, BDH, HiMedia, Aarti Drugs LTd., Fluka-Garantie, Fluka, Merck, Sigma, Ajenta Pharm, Intron Biotech, and PSI) without additional purification.

2.2. Methods

2.2.1. Synthesis of 2-amino-4-(methylthio) butanoic(bis(2-(2-methyl -5-nitro-1Himidazol -1-yl) ethyl) boric)anhydride (MBIB)

The BIB ligand was synthesized in our previous work [from metronidazole (0.1 g) and boric acid (0.0180 g) in a 2:1 mole ratio and refluxed in H_2O for 8 hours]. The solution of BIB (0.1 gm, 0.276 mmol) in distilled water (8 mL) was added to a solution of methionine (0.0404 g, 0.2718 mmol) in distilled water (4 mL). The mixture was then stirred in a water bath at 42 °C for 8 hours. Part of the solvent was evaporated, and the product was collected using an ice bath and dried in an oven at 80 °C.

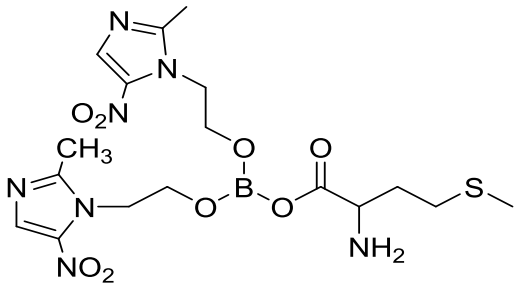

Figure 1: The structure of the MBIB ligand

2.2.2. Synthesis of MBIB complexes with Ni(II), Cu(II) and Pt(IV))(C_1, C_2 and C_3)

A solution of MBIB (0.1 g, 0.2004 mmol) in distilled water (5 mL) and metal salt (0.0238, 0.0170 and 0.0486 gm (0.1000 mmol)) of [($NiCl_2.6H_2O$), ($CuCl_2.2H_2O$) and (K_2PtCl_6)], respectively in distilled water (2 mL) was added. The mixture was then heated to reflux for 5

hours. Part of the solvent was evaporated, and the product was collected using an ice bath and dried in an oven at 80 °C.

2.2.3. Anti-biofilm activity

2.2.3.1. Minimum inhibitory concentrations

MIC: The minimum inhibition concentration of the ligand and complexes was measured in concentrations (32, 64, 128, 256, 512 and 1024 mg/mL) using the microdilution broth method in microtiter plates.

2.2.3.2. Biofilm formation

The biofilm formation was evaluated in a polystyrene 96-well microplate. Bacterial strains were cultivated overnight for 24 hours at 37 °C in broth culture with glucose (0.2%), both in the presence and absence of MIC concentrations of chemical compounds. After removing the medium, biofilm-containing wells were washed three times with normal saline before being fixed with methanol (200 µL, 99%). The microplate was washed three times with distilled water, dyed for 15 minutes with crystal violet (200 µL, 0.1%), and dried at room temperature. After the dye that adhered to the biofilm was solubilized in absolute ethanol (200 µL), the absorbance was measured at 630 nm. The experiments were repeated three times, and the data were shown as absorption means [8,9].

2.2.4. Anticancer activity

To evaluate the cytotoxic effect, a 96-well plate was used for the MTT cell viability assay. The cell-lines were seeded (1×10^4 cells/ well). Cells were treated with the studied compounds after 24 hours. The effectiveness of the anti-cancer treatment was studied through the literature [10], and absorbance at 575 nm was evaluated.

3. Results and discussion

The physical and analytical data are consistent with the proposed structures of the compounds in the study (Table 1).

Table 1: Data from analysis as well as the physical characteristics of MBIB ligand and its metal complexes

Compound	The formula	Color	Yield (%)	Melting point (°C)	Molecular wight (g/mol)	Calculated (Fou.)				Metal content (%)	Chloride content (%)
						C%	H%	S%	N%		
MBIB	$C_{17}H_{26}N_7O_8BS$	White	85	170-172	498.8	40.89 (40.09)	5.21 (5.81)	6.41 (5.68)	19.64 (19.61)	-	-
C_1(Ni)	$[C_{34}H_{54}N_{14}B_2O_{17}S_2NiCl]Cl$	Green	70	160-162	1145.29	35.62 (36.59)	4.71 (4.87)	5.58 (4.67)	17.11 (18.03)	5.12 (4.74)	6.19 (7.45)
C_2 (Cu)	$[C_{34}H_{54}N_{14}O_{17}B_2S_2CuCl]Cl$	Dark green	98	154-156	1150.14	35.47 (36.29)	4.69 (5.20)	5.56 (5.18)	16.27 (17.04)	5.52 (4.89)	6.17 (5.32)
C_3 (Pt)	$[C_{34}H_{56}N_{14}B_2O_{18}S_2Pt]4Cl.4H_2O$	Brown	70	136-138	1442.68	28.28 (27.42)	4.43 (3.61)	4.43 (5.27)	13.58 (13.83)	-	9.84 (9.18)

Table 2: The name of MBIB and proposed formula for its metal ion complexes

Compound	Proposed formula	Compound name
MBB	$C_{17}H_{26}N_7O_8BS$	2-Amino-4-(methylthio) butanoic(bis(2-(2-methyl-5-nitro-1*H*-imidazol-1-yl)ethyl)boric)anhydride
C_1	$[(L_2)_2Ni(H_2O)Cl].Cl$	[Aaqua chloro-bis{2-amino-4-(methylthio) butanoic(bis(2-(2-methyl-5-nitro-1*H*-imidazol-1-yl)ethyl) boric)anhydride}nickel(II)]chloride
C_2	$[(L_2)_2Cu(H_2O)Cl].Cl$	[Aqua chloro-bis {2-amino-4-(methylthio) butanoic(bis(2-(2-methyl 5-nitro-1*H*-imidazol-1-yl)ethyl) boric) anhydride}copper(II)]chloride
C_3	$[(L_2)_2Pt(H_2O)_2].4Cl.6H_2O$	[Diaqua bis{2-amino-4-(methylthio) butanoic(bis(2-(2-methyl-5-nitro-1*H*-imidazol-1-yl)ethyl) boric)anhydride}platinium(IV)]tetrahydrate chloride

3.1. FT-IR spectroscopy

The FT-IR spectrum of the MBIB ligand showed a change in the position of OH band compared with the original BIB ligand because of the insertion of methionine moiety (Table 3) [11]. A new band appears in the ligand and complex spectra at 1612-1622 cm^{-1}, which is assigned to the C=O group [12]. In comparison to BIB, the band of C=N for the ligand and its complexes did not change [2,12]. The spectra of the ligand and its complexes appeared band at 1473-1487 cm^{-1} which is due to the B-O band [12,14]. Low-frequency bands appeared in complex spectra due to M-O, M-S, M-N, and M-Cl stretching vibrations, as shown in Figures 3-6 [2,12,15].

Table 3 : FT-IR spectral data (υ, cm^{-1}) of the MBIB ligand and it complexes

Compound	OH	NH_2	H_2O lattice (coordinate)	C=O	C=N	B-O	M-O	M-S	M-N	M-Cl
BIB	3431	-	-		1535	1487	-	-	-	-
MET	3436	-	-	1608	-	-	-	-	-	-
MBIB	-	3398 3220	-	1612	1537	1485	-	-	-	-
C_1(Ni)	-	3407 3224	3380 767 588	1622	1535	1473	422	-	-	351
C_2(Cu)	-	3411 3226	3282 703 624	1620	1535	1473	426	-	-	335
C_3(Pt)	-	3377 3145	342 3398 835 680	1612	1535	1485	-	345	314	-

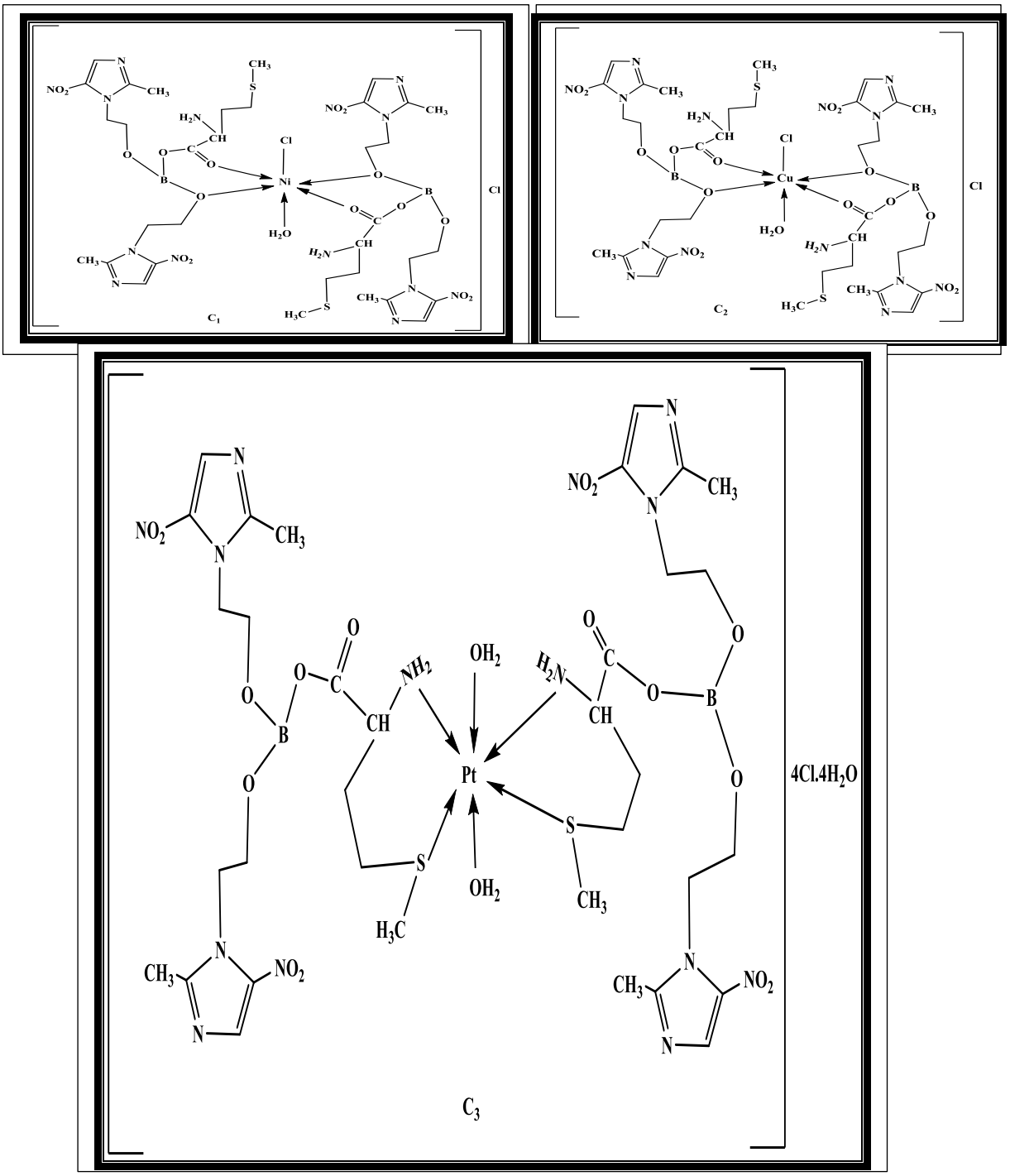

Figure 2: The suggested structures of synthesized complexes

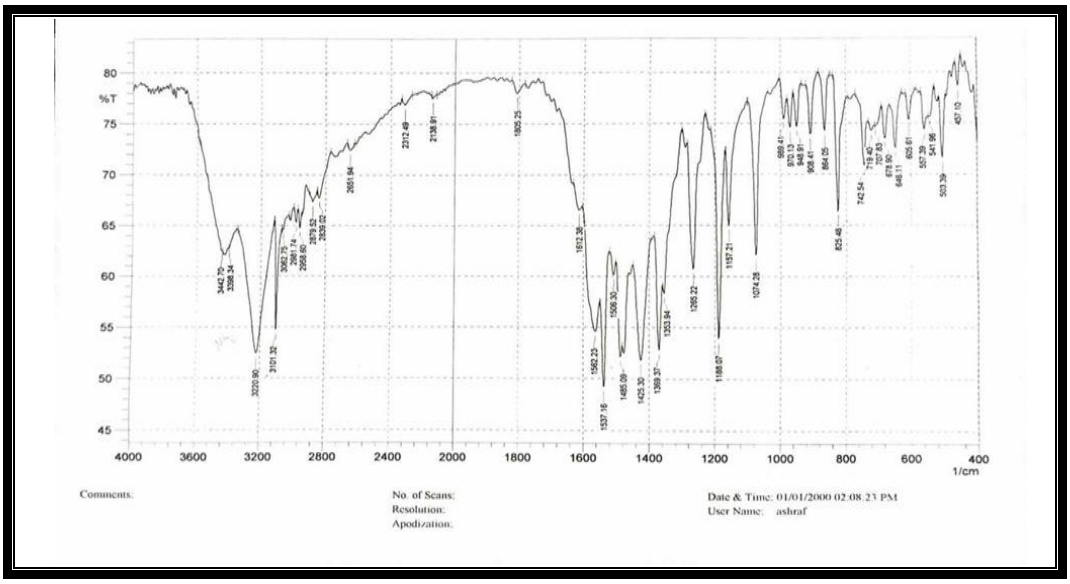

Figure 3: FT-IR spectrum of the MBIB ligand

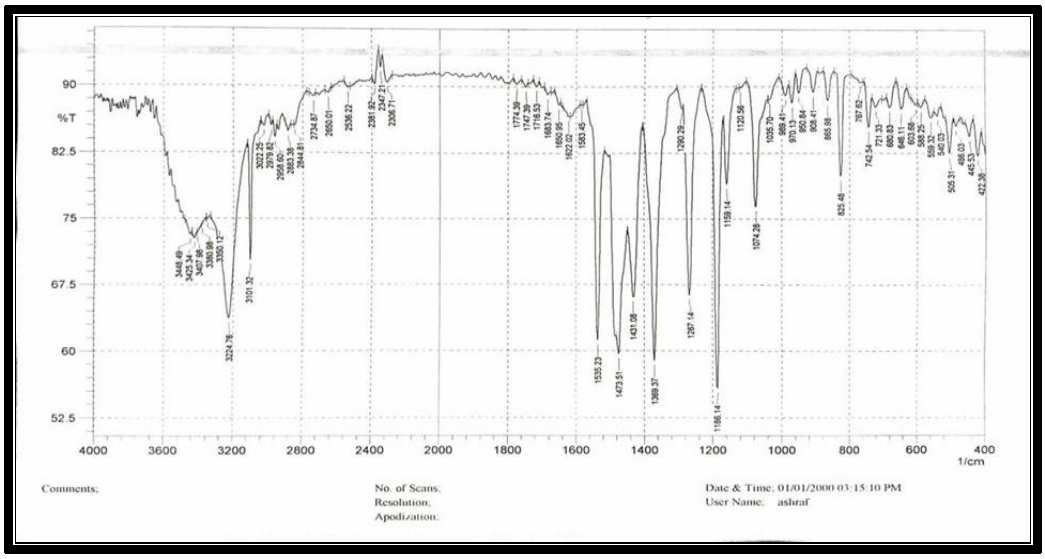

Figure 4: FT-IR spectrum of the nickel(II) complex C_1

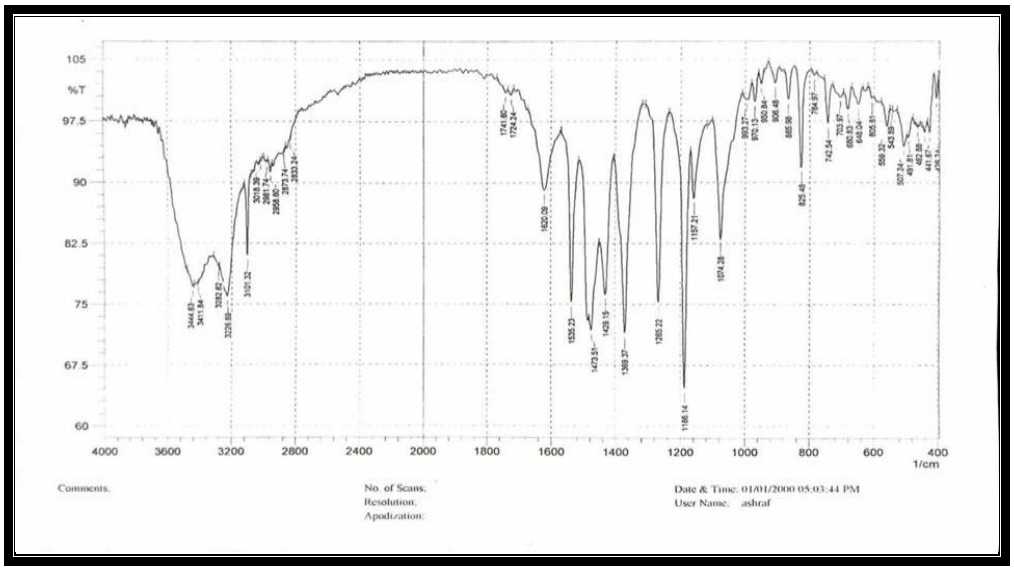

Figure 5 - FT-IR spectrum of the copper(II) complex C_2

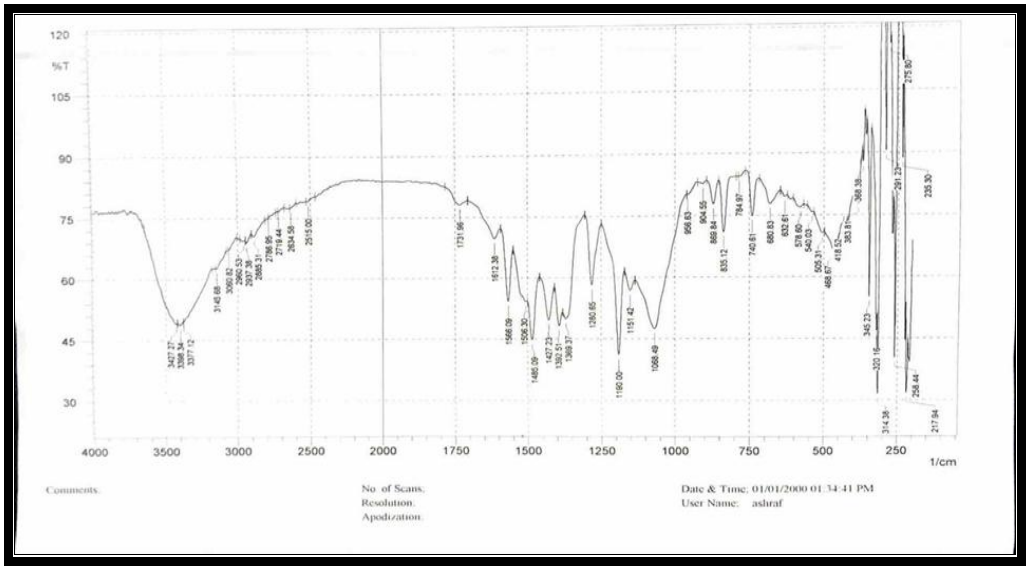

Figure 6: FT-IR spectrum of the platinum (IV) complex C_{33}

3.2. ^{1}H NMR spectroscopy

The ^{1}H NMR spectrum of the MBIB ligand is shown in Figure 7, and the data are consistent with the literature [12,14,18, and 19].

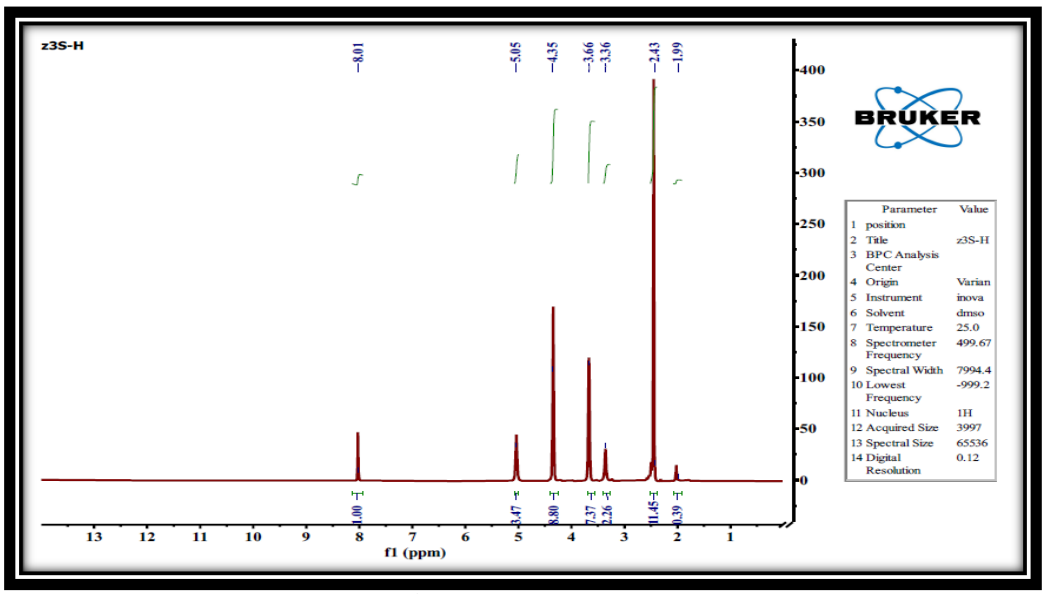

Figure 7 - ^{1}H NMR spectrum of MBIB

3.3. Thermogravimetric analysis (TGA)

The TG analysis was carried out under argon gas at a heating rate of 10 C/min. and a temperature range of 25-800 ^{o}C. Using this technique, the structures were characterized, as well as the thermal stabilities of the synthesized compounds. In the following order, the MBIB ligand and its complex's thermal stability were increased: (C_1 > C_3 > MBIB > C_2) (Table 4) [2]. Thermal decomposition was utilized to confirm the structures where the information of degradation exhibits high agreed with found mass loss and calculation, which confirms the proposed structures of synthesized compounds. The thermograms of the MBIB ligand and platinum complex C_3 are shown in Figures 8 and 9.

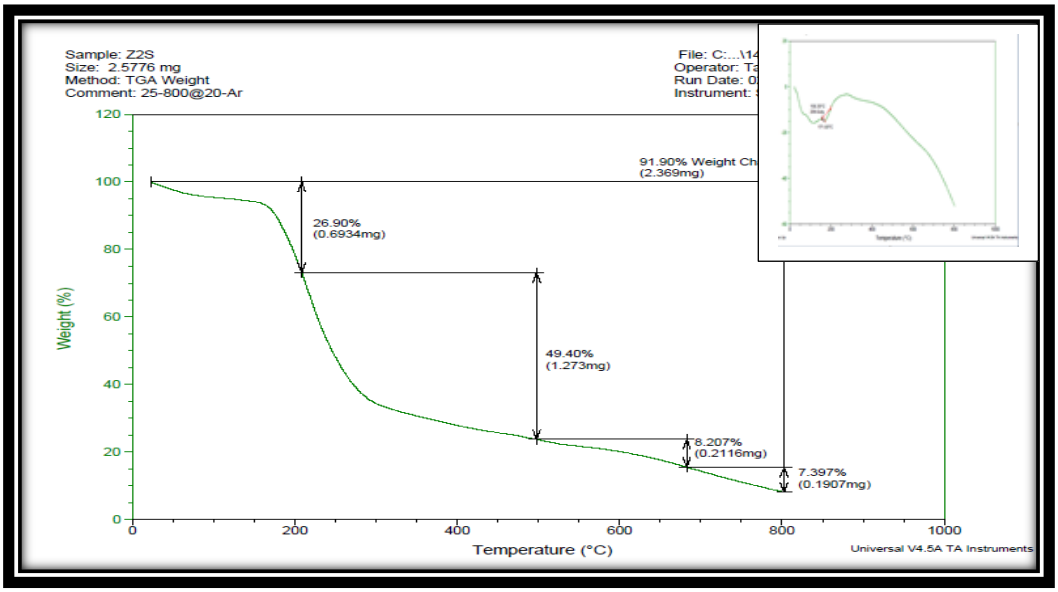

Figure 8: Thermogram of the MBIB ligand

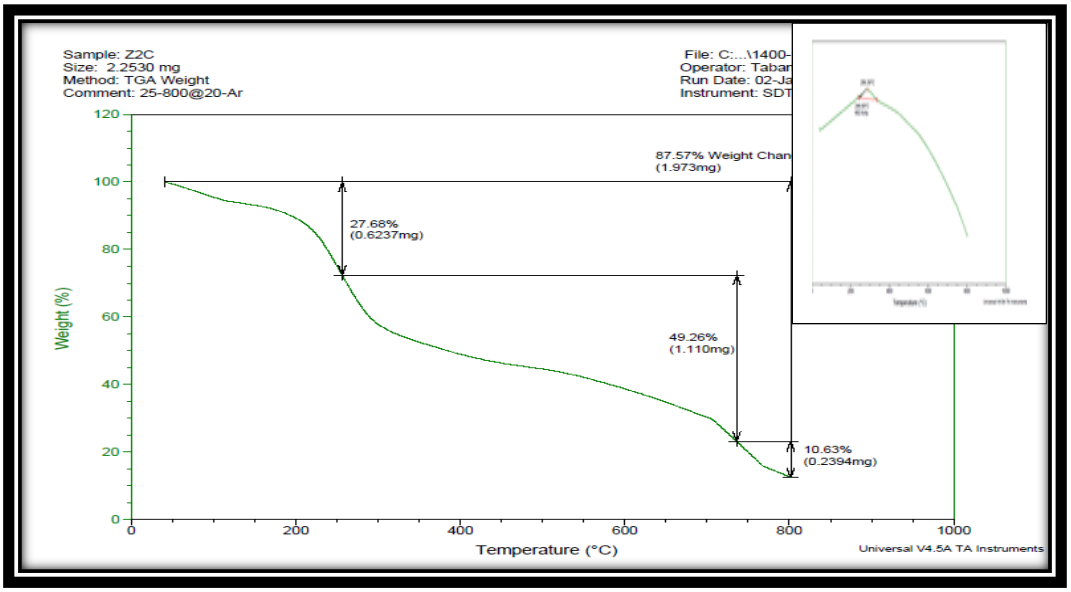

Figure 9: Thermogram of platinum complex C_3.

Table 4: TGA of MBIB ligand and their complexes

Compounds	Molecular formula (molecular weight) g/mole	Step	Temperature rang of the decomposition (°C)	DSC (°C)	Suggested formula of loss	Mass loss (%)	
						Calculated	Found
MBIB	$C_{17}H_{26}N_7O_8BS$ 498.8	1	25-208	158.35 (Exo)	$N_3C_4H_8O_2$	26.06	26.90
		2	208-496	171.93 (Exo)	$C_9H_{14}N_4O_2S$	49.11	49.40
		3	496-685	-	C_2OH	8.219	8.207
		4	685-800	-	C_2O	8.019	7.397
		Residue	>800		BO_2	8.58	8.10
C_1	$[C_{34}H_{54}N_{14}B_2O_{17}S_2NiCl]Cl$ 1145.29	1	25-265	158.29 (Exo)	$H_2O+2Cl+N_6O_7C_{12}H_{16}B$	39.79	39.67
		2	265-800	289.60 (Exo)	$N_7O_8C_{17}H_{11}B+S$	43.55	43.05
		Residue	>800	-	$C_5H_{10}NS$ Ni O	16.64	17.28
C_2	$[C_{34}H_{54}N_{14}O_{17}B_2S_2CuCl]Cl$ 1150.14	1	25-263	230.46 (Exo)	$H_2O+2Cl+N_6O_7C_{17}H_{26}BNS$	49.91	49.12
		2	263-800	259.71 (Exo)	$N_7O_8C_{17}H_{26}CuS$	47.95	48.90
		Residue	>800	-	BO	2.33	1.97
C_3	$[C_{34}H_{56}N_{14}B_2O_{18}S_2$ Pt]4Cl.4H_2O 1442.68	1	25-257	246.69 (Exo)	$6H_2O+4Cl+2NO_2+CH_3+S$	26.96	27.68
		2	257-741	286.39 (Exo)	$N_{11}C_{28}O_{10}H_{39}B_2$	49.25	49.26
		3	741-800	-	$C_6H_{10}NSO_2$	10.25	10.63
		Residue	>800	-	Pt	13.52	12.43

3.4. UV-Vis spectral studies

All the details of the spectra are listed in Table 5. The spectrum of MBIB (Figure 10) exhibited the bands in the region of 323 nm (30959 cm^{-1}), which were assigned to the π -π* transition [11]. The spectrum of the Ni(II) complex (Figure 11) exhibited a shift in the position of the π -π* transition. Double bands were at 964 nm (10373 cm^{-1}), 670 nm (14925 cm^{-1}), which noticed $^3A_2g \rightarrow {}^3T_2g$ and $^3A_2g \rightarrow {}^3T_1g(P)$ transition, respectively [21]. The magnetic moment of the nickel complex (C_1) was 3.12 BM, and this value of M_{eff} agreed with octahedral geometry [22,23]. The spectrum of the copper complex (Figure 12) exhibited a shift in the position of the π -π* transition. The paramagnetic C_2 complex showed two-bands at 976 nm (10245 cm^{-1}), and 695 nm (14388 cm^{-1}). These bands refer to the $^2B_1g \rightarrow {}^2A_1g$ and $^2B_1g \rightarrow {}^2B_2g$ transitions, respectively. The magnetic moment of the copper complex (C_2) was 2.48 BM, and the value of M_{eff} demonstrated distorted octahedral geometry [24]. The

spectrum of Pt(IV) complexes is shown in Figure 13, which shows a shift in the π -π* transition. The electronic spectrum of diamagnetic C_3Pt showed a double band at 970 nm (10309 cm^{-1}) and 540 nm (18518 cm^{-1}), that also refer to the $^1A_1g \rightarrow {}^1T_1g$ and $^1A_1g \rightarrow {}^3T_1g(H)$ transitions of an octahedral Pt(IV) complex [25,26]. The MC measurements of C_1, C_2, and C_3 complexes in distilled water showed that the complexes C_1 and C_2 are 1:1. Complex C_3 has a 1:3 ratio of electrolyte properties [27,28].

Table 5: Electronic transitions of the MBIB ligand and its complexes, proposed geometry, molar conductivity, and magnetic susceptibility

Compound	ג nm (cm^{-1})	Assignment	Molar conductivity ($S.cm^2.mol^{-1}$) in H_2O	M_{eff} (B.M)	Geometry
MBIB	323(30959)	π -π*	-	-	-
C_1(Ni)	323(30959)	π -π*	142	3.12	Octahedral
	670(14925)	$^3A_2g \rightarrow {}^3T_1g(F)$ (υ_2)			
	964(10373)	$^3A_2g \rightarrow {}^3T_2g$ (υ_1)			
C_2(Cu)	352(28409)	π -π*	159	2.48	Distorted octahedral
	695(14388)	$^2B_1g \rightarrow {}^2B_2g$ (υ_2)			
	976(10245)	$^2B_1g \rightarrow {}^2A_1g$ (υ_1)			
C_3(Pt)	326(30674)	π -π*	559	dia	Octahedral
	450(22222)	$^1A_1g \rightarrow {}^3T_2g$ (υ_3)			
	540(18518)	$^1A_1g \rightarrow {}^3T_1g(H)$ (υ_2)			
	970(10309)	$^1A_1g \rightarrow {}^1T_1g$ (υ_1)			

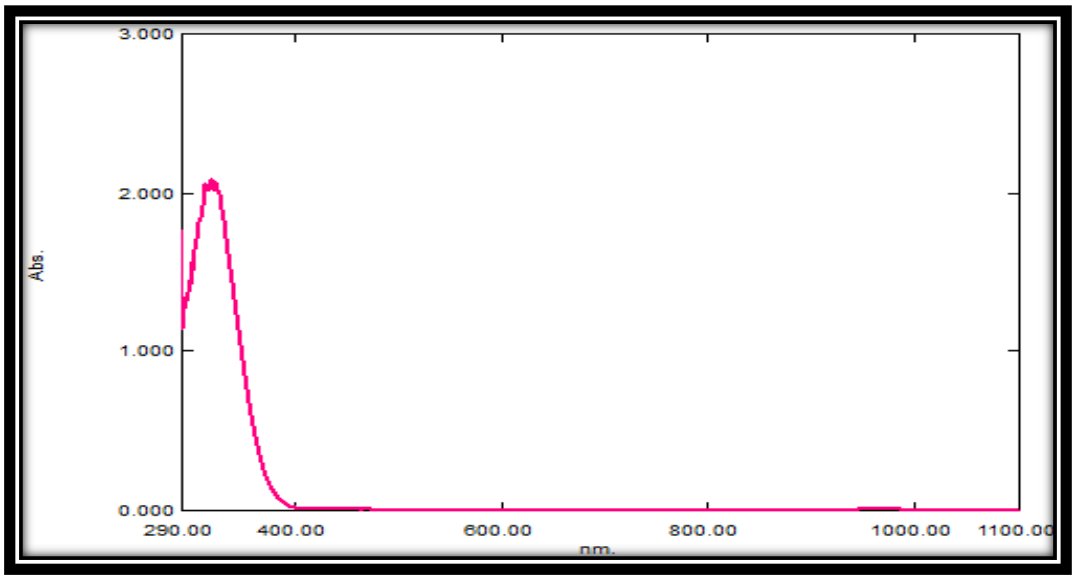

Figure 10: UV-Vis spectrum of the MBIB ligand

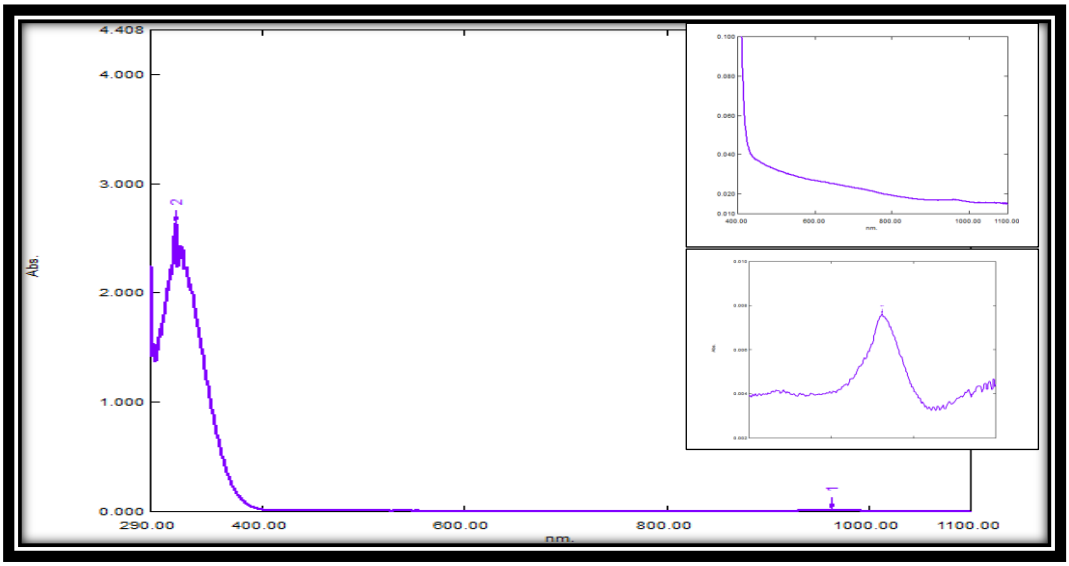

Figure 11: UV-Vis spectrum of the nickel(II)complex C_1

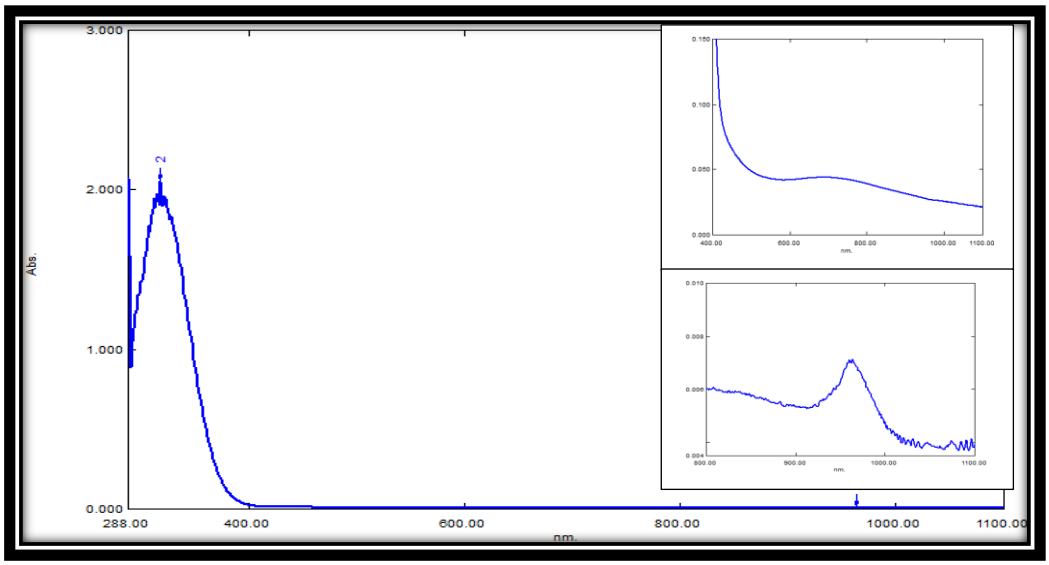

Figure 12: UV-Vis spectrum of the copper(II)complex C_2

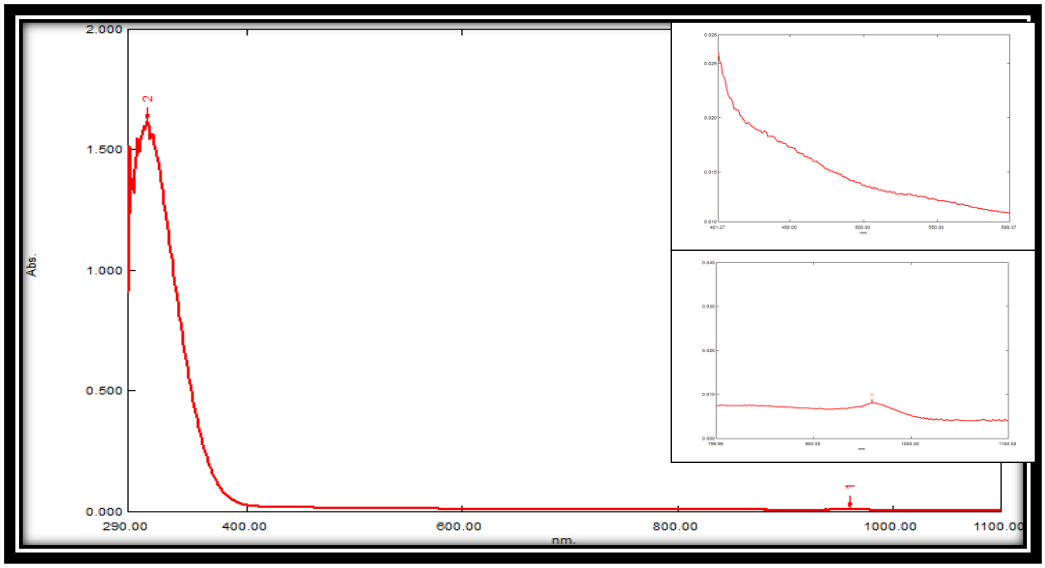

Figure 13: UV-Vis spectrum of the platinum(IV) complex C_3

3.5. Anti-cancer activity

Metronidazole and MBIB ligand were evaluated for their ability to inhibit human breast cancer (MCF-7) cells by the 3-(4,5-dimethylthiazol-2-yl)-2,5-diphenyltetrazolium bromide (MTT) assay technique (Figures 14 and 15). Different concentrations of metronidazole and MBIB ligand were used in the MTT assay to determine cell viability and the inhibition rate of the tumor cell line. In comparison with the normal cell line WPL-68, the percentage of viable cells was calculated, as shown in Tables 6 and 7.

Table 6: Cytotoxicity effects of metronidazole on MCF-7 and WRI-68 cells after 24 hours incubation at 37 °C

Cell line	Concentration (µg/mL)						IC_{50} (µg/mL)	P value
	200.00	100.00	50.00	25.00	12.50	6.25		
MCF-7	55.67± 3.64	61.00± 1.48	76.08± 1.77	89.82± 2.34	92.86± 4.65	95.02± 1.45	53.29	<0.0001
WRL	77.28± 1.62	87.96± 1.51	92.13± 1.56	95.41± 0.37	95.79± 0.71	94.91± 2.20	297.4	

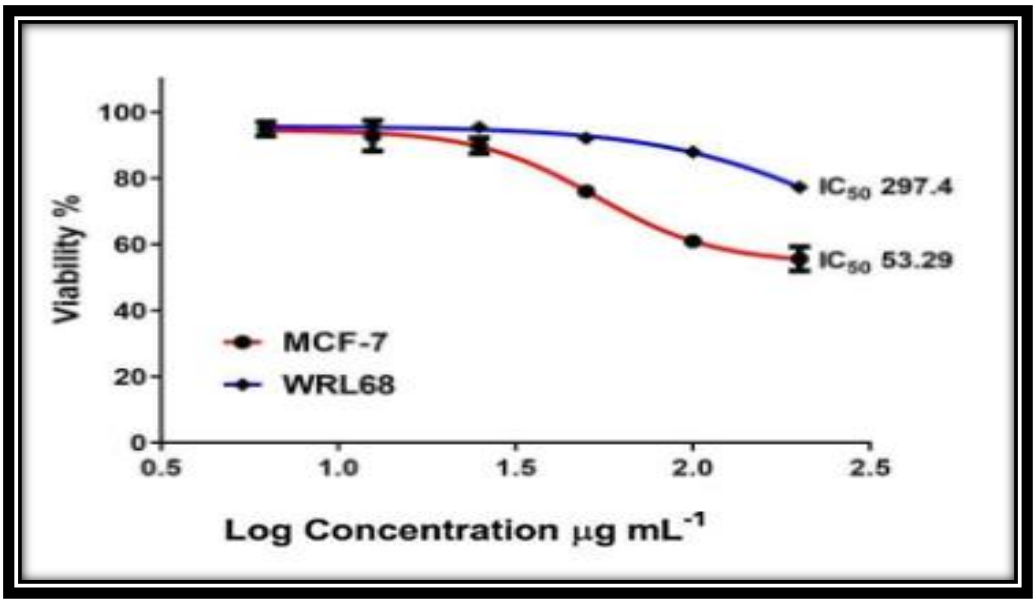

Figure 14: The cytotoxicity of metronidazole ligand on MCF-7 cells (Log for the original concentration), after 24 hours of incubation at 37 °C

Table 7: Cytotoxicity effects of MBIB ligand on MCF-7 and WRI-68 cells after 24 hours incubation at 37 °C

Cell line	Concentration (µg/mL)						IC_{50} µg/ml	P value
	200.00	100.00	50.00	25.00	12.50	6.25		
MCF-7	64.56± 2.78	71.70± 1.25	93.76± 3.06	93.62± 1.89	95.65± 1.17	95.25± 0.92	83.38	<0.0001
WRL	73.11± 4.41	82.73± 1.39	93.60± 2.10	94.56± 0.53	95.22± 0.82	95.18± 0.41	96.83	

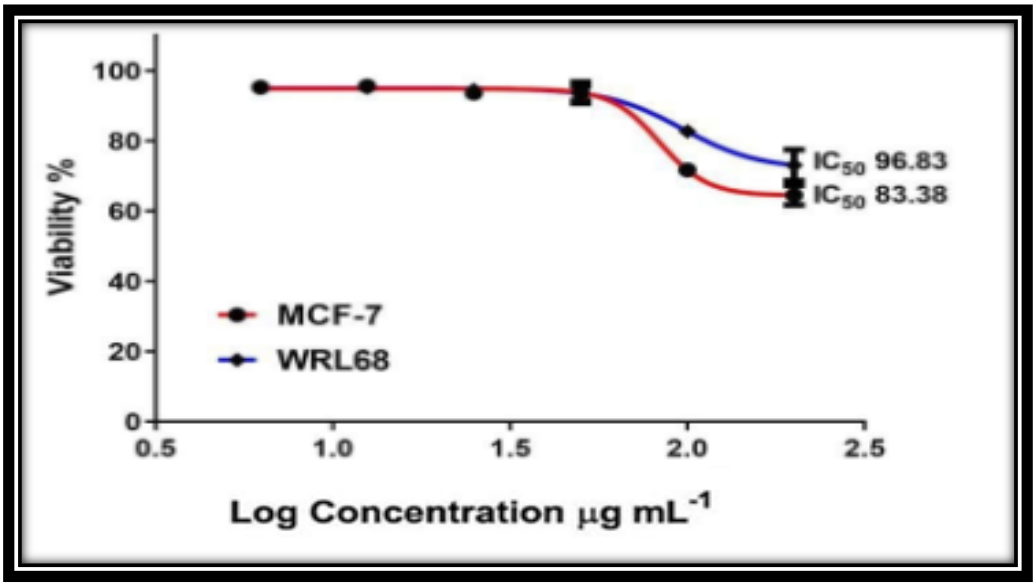

Figure 15: The cytotoxicity of MBIB ligand on MCF-7 cells (Log for the original concentration), after 24 hours of incubation at 37 °C

According to the results, MBIB ligand has been killed the least by metronidazole. This may be because methionine is present, which links to several important metabolic pathways that play key roles in epigenetics, nuclear functions, detoxification, and cellular membranes [29].

3.6. Anti-Biofilm (biological activity)

Assessing biofilm formation of P. aeruginosa isolates

Isolates of *Pseudomonas aeruginosa* may be able to develop biofilms on microtiter plates (Table 8). The results suggested that *P. aeruginosa* (40.0%) isolates produced strong biofilms, while 33.3 and 26.6% of isolates produced moderate and weak biofilms, respectively [30-33].

Table 8: Biofilm intensity based on an estimated cutoff value* of *P. aeruginosa* isolates

ID Biofilm	Intensity	OD630 limits number of isolates	Number of isolates	Percentage (%)
1	Non-biofilm producer	<0.05	0	0
2	Weak	0.05 - 0.10	4	26.6
3	Moderate	0.10 - 0.20	5	33.3
4	Strong	≥ 0.20	6	40.0

3.7. Determination of the MIC and sub-mic for(metronidazole, MBIB and all complexes)

MIC is defined as the lowest concentration of a substance tested that prevented the blue to pink change of resazurin [34]. The broth microdilution method was used to determine the MIC of MTN, MBIB, and all complexes in a 96-well microtiter plate. The susceptibility of an isolated *P. aeruginosa* with higher biofilm formation proberity (*P. aeruginosa* no. 5) against MTN, MBIB, and all complexes was tested by determining the MIC using microtiter plates. The results revealed that the MIC of MTN, C_2Cu, C_3Pt complexes which can inhibit bacterial growth, was 1024 µg/mL, and the MIC of MBIB ligand was 512 µg/mL, but C_1Ni had no inhibitory effect on bacterial growth. The MIC are shown in Table 9 and Figure 16.

Table 9: The MIC and sub-MIC of MTN, MBIB, and all complexes against *P. aerougenosa* isolates

Compound	**compound code**	***P. aerougenosa* isolates**	MIC (µg/mL)	**Sub MIC (µg/mL)**
MTN	As	P_5	1024	512
MBIB	As_1	P_5	512	256
C_1Ni	As_4	P_5	inactive	inactive
C_2Cu	As_2	P_5	1024	512
C_3Pt	As_3	P_5	1024	512

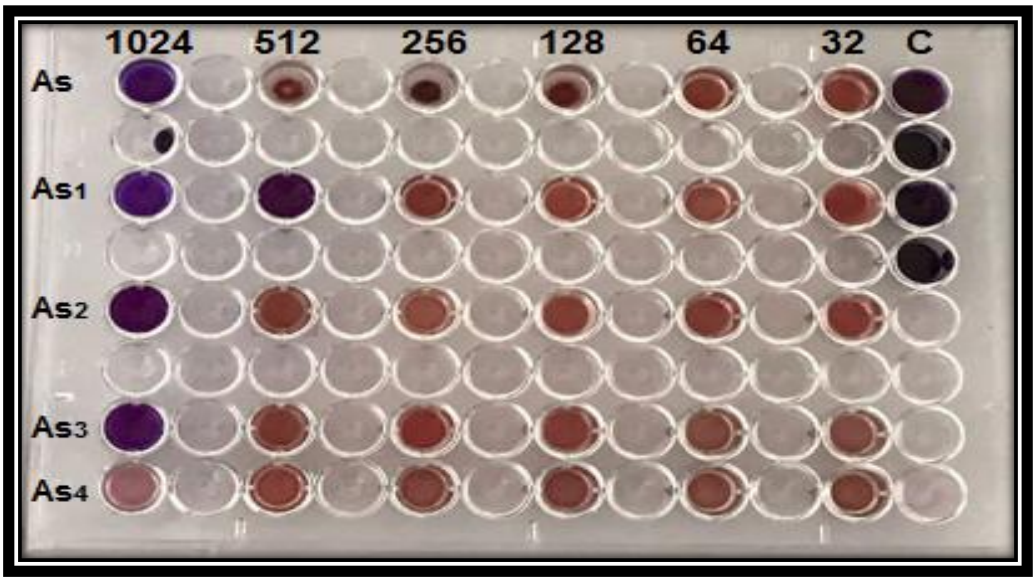

Figure 16: The MIC of MTN, MBIB and all complexes against *P. aerougenosa.*

3.8. Antibiofilm activity of MTN, MBIB, and effective complexes

The MTN, MBIB, and effective complexes were evaluated for their anti-biofilm activity. These compounds exhibited anti-biofilm activity against the tested bacterial isolate (*P. aerougenosa*), and anti-biofilm activity against them before the biofilm formation showed various degrees of inhibition. It is markedly evident that biofilm was significantly reduced ($P< 0.001$), evaluated by the microtiter plate assay method as shown in Table 10.

Table 10: Anti-biofilm activity of MTN, MBIB and effective complexes sub-MIC

Compound code	Bacteria	**OD**	**Before treatment**	**After treatment**	***P***
MTN	5	Mean± SD	0.492±0.045	0.277±0.068	< 0.001
MBIB	5	Mean± SD	0.492±0.045	0.258±0.099	< 0.001
C_2Cu	5	Mean± SD	0.492±0.045	0.201±0.091	< 0.001
C_3Pt	5	Mean± SD	0.492±0.045	0.214±0.079	< 0.001

The MTN, MBIB, and effective complexes succeeded in preventing them from forming biofilm, and most of them kill live cells inside the biofilm. Metals such as copper and platinum are used as anti-bacterial agents [35].

4. Conclusion

The new MBIB ligand was synthesized *via* the reaction of methionine with the BIB ligand. Its metal complexes with Ni(II), Cu (II), and Pt(II) were also synthesized (MBIB:M) in a 2:1

mole ratio. All synthesized compounds were characterized, and the suggested structure utilizes spectral and physicochemical techniques. The results revealed that all complexes have octahedral geometry and an electrolyte character. The biological results revealed that all the prepared compounds had excellent anti-biofilm activity against bacteria (*Pseudomonas auroginosa gram-negative*) except for C_1(Ni), which is inactive against the same bacteria. The synthesized MBIB ligand has less activity against human breast cancer (MCF-7) cells than metronidazole**.**

References

[1] L. Zhang, X. M. Peng, G. L. Damu, R. X. Geng, and C. H. Zhou, "Comprehensive review in current developments of imidazole-based medicinal chemistry," *Medicinal research reviews,* vol. 34, no. 2, pp. 340-437, 2014.

[2] A. E. Ali, G. S. Elasala, and R. S. Ibrahim, "Synthesis, characterization, spectral, thermal analysis and biological activity studies of metronidazole complexes," *Journal of Molecular Structure,* vol. 1176, pp. 673-684, 2019.

[3] E. Ezzeldin and T. M. El-Nahhas, "New analytical method for the determination of metronidazole in human plasma: Application to bioequivalence study," *Tropical Journal of Pharmaceutical Research,* vol. 11, no. 5, pp. 799-805, 2012.

[4] R. Pal, "Boric acid in organic synthesis: scope and recent developments," *ARKIVOC: Online Journal of Organic Chemistry,* vol. 2018, pp. 1-26, 2018.

[5] S. S. Gujral, "UV-Visible spectral analysis of boric acid in different solvents: a case study," *International Journal of Pharmaceutical Sciences and Research,* vol. 6, no. 2, pp. 830-834, 2015.

[6] T. Willke, "Methionine production - a critical review," *Applied Microbiology and Biotechnology,* vol. 98, no. 24, pp. 9893-9914, 2014.

[7] D. Wanders, K. Hobson, and X. Ji, "Methionine restriction and cancer biology," *Nutrients,* vol. 12, no. 3, pp. 684-698, 2020.

[8] F. Hemmati, R. Salehi,R. Ghotaslou, H. S. Kafil, A. Hasani, P. Gholizadeh, and A. M. Rezaee , "The assessment of antibiofilm activity of chitosan-zinc oxide-gentamicin nanocomposite on Pseudomonas aeruginosa and Staphylococcus aureus," *International Journal of Biological Macromolecules,* vol. 163, pp. 2248-2258, 2020.

[9] H. J. F. Al-Mathkhury, A. S. Al-Dhamin, and K. L. Al-Taie, "Antibacterial and antibiofilm activity of flaxseed oil," *Iraqi Journal of Science,* vol. 57, no. 2B, pp. 1086-1095, 2016.

[10] O. Ogwuegbu Martin, E. C. Kenechukwu, O. C. Stanley, E. N. Patricia, and E. C. Ebere, "Stoichiometric Determination of Fe (II), Ni (II) and Cu (II) Complexes of Metronidazole," vol. 3, pp. 25-29, 2019.

[11] C. Giromini, M. Tretola, C. Cristiani, E. Finocchio, P. Silacci, S. Panseri, M. Dell'Anno, A. Baldi, and L. Rossi, "Evaluation of the Absorption of Methionine Carried by Mineral Clays and Zeolites in Porcine Ex Vivo Permeability Models," *Applied Sciences,* vol. 11, no. 14, pp. 6384-6394, 2021.

[12] A. A. Al-Jibori, S. A. Al-Jibori, and A. S. Al-Janabi, "Palladium (II) and platinum (II) mixed ligand complexes of metronidazole and saccharinate or benzisothiazolinonate ligands, synthesis and spectroscopic investigation," *Tikrit Journal of Pure Science,* vol. 24, no. 6, pp. 26-32, 2019.

[13] S. Ramukutty and E. Ramachandran, "Crystal growth by solvent evaporation and characterization of metronidazole," *Journal of crystal growth,* vol. 351, no. 1, pp. 47-50, 2012.

[14] R. H. Georgieva, P. S. Vassileva, A. K. Detcheva, D. K. Voykova, T. I. Gerganova, and Y. Y. Ivanova, "Synthesis, characterization and adsorption properties of nanostructured hybrid materials modified by boron and zirconium," *Central European Journal of Chemistry,* vol. 10, no. 5, pp. 1484-1494, 2012.

[15] J. Obaleye and A. Lawal, "Synthesis, characterization and antifungal studies of some metronidazole complexes," vol. 11, no. 4, pp. 15-18, 2007.

[16] A. Waszczykowska, D. Żyro, P. Jurowski, and J. Ochocki, "Effect of treatment with silver (I) complex of metronidazole on ocular rosacea: Design and formulation of new silver drug with potent antimicrobial activity," *Journal of Trace Elements in Medicine and Biology,* vol. 61, p. 126531, 2020.

[17] E. Monteagudo, A. Virgili, T. Parella, and M. Pérez-Trujillo, "Chiral recognition by dissolution DNP NMR spectroscopy of 13C-labeled DL-methionine," *Analytical chemistry*, vol. 89, no. 9, pp. 4939-4944, 2017.

[18] M. S. Shoshan, D. E. Shalev, W. Adriaens, M. Merkx, T. M. Hackeng, and E. Y. Tshuva, "NMR characterization of a Cu (I)-bound peptide model of copper metallochaperones: Insights on the role of methionine," *Chemical Communications*, vol. 47, no. 22, pp. 6407-6409, 2011.

[19] S. Dong, Y. Jiang, G. Qin, L. Liu, and H. Zhao, "Methionine-based pH and oxidation dual-responsive block copolymer: Synthesis and fabrication of protein nanogels," *Biomacromolecules*, vol. 21, no. 10, pp. 4063-4075, 2020.

[20] M. Kundu, S. Saha, and M. N. Roy, "Evidences for complexations of β-cyclodextrin with some amino acids by 1H NMR, surface tension, volumetric investigations and XRD," *Journal of Molecular Liquids*, vol. 240, pp. 570-577, 2017.

[21] K. J. Al-Adilee, K. A. Abedalrazaq, and Z. M. Al-Hamdiny, "Synthesis and Spectroscopic Properties of Some Transition Metal Complexes with New Azo-Dyes Derived From Thiazole and Imidazole," *Asian Journal of Chemistry*, vol. 25, no. 18, pp. 10475-10481, 2013.

[22] N. Ahmad, N. Abdullah, and M. A. Malik, "Synthesis, structural and magnetic studies of dinuclear complexes with oxo-homoscorpionate borate ligand," *World Applied Sciences Journal*, vol. 17, no. 2, pp. 148-156, 2012.

[23] A. M. N. Khaleel, "Synthesis and Characterization of Trihydro mono and Dihydrobis (indole-3-acetic acid) Borate Ligands and Some of Their Metal Complexes," *Iraqi Journal of Science*, vol. 56, no. 4A, pp. 2762-2772, 2015.

[24] A. J. Abdul-Ghani and A. Khaleel, "Synthesis and characterization of new schiff bases derived from N (1)-substituted isatin with dithiooxamide and their co (II), Ni (II), Cu (II), Pd (II), and Pt (IV) complexes," *Bioinorganic Chemistry and Applications*, vol. 2009, pp. 1-12, 2009.

[25] N. A. Hussein and A. K. Abbas, "Synthesis, spectroscopic characterization and thermal study of some transition metal complexes derived from caffeine azo ligand with some of their applications," vol. 4, no. 1, pp. 66-92, 2022.

[26] A. M. N. Khaleel and M. I. Jaafar, "Synthesis and characterization of boron and 2-aminophenol Schiff base ligands with their Cu(II) and Pt(IV) complexes and evaluation as antimicrobial agents," *Oriental Journal of Chemistry*, vol. 33, no. 5, pp. 2394-2404, 2017.

[27] W. J. Geary, "The use of conductivity measurements in organic solvents for the characterisation of coordination compounds," *Coordination Chemistry Reviews*, vol. 7, no. 1, pp. 81-122, 1971.

[28] T. Yoshino, "Laboratory electrical conductivity measurement of mantle minerals," *Surveys in Geophysics*, vol. 31, no. 2, pp. 163-206, 2010.

[29] P. Kaiser, "Methionine dependence of cancer," *Biomolecules*, vol. 10, no. 4, pp. 568-583, 2020.

[30] N. T. mohammed Jaddoa and H. J. F. Al-Mathkhury, "Biofilm Shows Independency form Hemolysin Genes Arsenal in Methicillin Resistant Staphylococcus Aureus," *Iraqi Journal of Science*, vol. 59, no. 4, pp. 2184-2194, 2018.

[31] M. A. R. H. Al-Sheikhly, L. N. Musleh, and H. J. Al-Mathkhury, "Gene Expression of pelA and pslA in Pseudomonas aeruginosa under Gentamicin Stress," *Iraqi Journal of Science*, vol. 61, no. 2, pp. 295-305, 2020.

[32] L. H. Mahdi, H. S. Jabbar, and I. G. Auda, "Antibacterial immunomodulatory and antibiofilm triple effect of Salivaricin LHM against Pseudomonas aeruginosa urinary tract infection model," *International journal of biological macromolecules*, vol. 134, pp. 1132-1144, 2019.

[33] L. H. Mahdi, A. R. Laftah, K. H. Yaseen, I. G. Auda, and R. H. Essa, "Establishing novel roles of bifidocin LHA, antibacterial, antibiofilm and immunomodulator against Pseudomonas aeruginosa corneal infection model," *International Journal of Biological Macromolecules*, vol. 186, pp. 433-444, 2021.

[34] I. Radojević, S. Vasić, L. Čomić, S. Trifunović, M. Mijajlović, M. Nikolić, and G. Radić, "Antibacterial and antibiofilm screening of new platinum (IV) complexes with some s-alkyl derivatives of thiosalicylic acid," *Kragujevac Journal of Science*, vol. 49, no. 39, pp. 137-143, 2017.

[35] M. L. Beeton, J. R. Aldrich-Wright, and A. Bolhuis, "The antimicrobial and antibiofilm activities of copper (II) complexes," *Journal of inorganic biochemistry*, vol. 140, pp. 167-172, 2014.